RT&A, No 3 (79)
Volume 19, September 2024

IMPROVING THE SPECTRAL EFFICIENCY IN DOWNLINK MULTIPLE USER MULTIPLE INPUT MULTIPLE OUTPUT TRANSMISSION FOR FIFTH GENERATION AND BEYOND WIRELESS COMMUNICATIONS

Abdulmujeeb Akajewole Masud, Donatus Uchechukwu Onyishi
•
Department of Electrical and Electronics Engineering
Federal University of Petroleum
Effurun, Nigeria
abdulmujeebakajewole@gmail.com, onyishi.donatus@fupre.edu.ng

Abstract

This research presents a solution in Multiple Input Multiple Output (MIMO) wireless systems to meet the growing demand for high data rates in cellular networks. Although MIMO systems offer greater capacity, the higher frequencies used have caused interference problems, especially for mobile User Equipment (UE). This research aims to reduce interference problems in the downlink of Multi-user MIMO (MU-MIMO) systems, with a specific focus on improving Quality of Service (QoS) metrics, such as outage probability and Signal-to-Interference plus Noise Ratio (SINR). Existing solutions to these challenges are complex due to the dynamic nature of the factors involved in modelling real-world scenarios. As such, an Improved Downlink MU-MIMO (ID-MU-MIMO) algorithm is developed as a solution to these problems. The ID-MU-MIMO method employs both single antenna users and multiple transmitter antennas. The performance of the suggested algorithm is compared to the IEEE 802.11ax standard specification and a previous research work for validation and evaluation. Performance measures considered to aid validation included outage probability, spectrum efficiency, and communication connection reliability. On this premise, the outcomes showed that the proposed ID-MU-MIMO scheme outperforms both the IEEE 802.11ax standard and current MD-MU-MIMO systems. In particular, compared to IEEE 802.11ax, the ID-MU-MIMO technique achieved a 7.71% reduction in interference. When compared to the performance of the random and uniform MD-MU-MIMO algorithms, the proposed ID-MU-MIMO scheme showed a reduction in interference in percentages of 8.90% and 2.28%, respectively. The ID-MU-MIMO scheme outpermed the random and uniform MD-MU-MIMO algorithms in terms of Signal-to-Interference Noise Ratio (SINR), outperforming them by 4.27% and 2.75%, respectively, and resource block use, outperforming them by 20.05% and 3.89%, respectively.

Keywords: ID-MU-MIMO, Interference, MU-MIMO, Resource Utilization, SINR

I. Introduction

The growing demand for wireless data, driven by the pervasive adoption of smart devices and mobile internet applications, is mirroring the exponential growth predicted by Martin Cooper's Law [1]. This law forecasts a doubling of wireless data usage every 2.5 years, a trend expected to accelerate in the coming years, with data rate requirements projected to surge by a staggering 5,000-fold by 2030 [2]. To address this growing demand, Fifth Generation (5G) technology emerged as a game-changer, surpassing the capabilities of its predecessor, Fourth Generation (4G), to meet the escalating needs [3]. One of its primary objective, as outlined in [4], is to achieve near-ubiquitous coverage while minimizing the likelihood of outages. This necessitates the development of innovative approaches that enhance spectral efficiency without compromising energy and bandwidth requirements [5]. Prominent standardization bodies, like the 3GPP and its affiliated groups, actively strive to establish standards that meet these objectives. These standards are designed to provide adaptable, easily accessible, and user-centric wireless data services, fulfilling the aforementioned commitments while adapting to evolving user requirements [6]. Consequently, technologies such as NOMA, massive MIMO, hybrid precoding, mm-wave, OFDM, beamforming, and D2D are utilized to enhance performance after data transmission [4], [7]. Since its inception in the era of 3G wireless networks, MIMO technology has continuously revolutionized the performance of wireless transceivers, enabling unprecedented data rates and spectral efficiency [8]. In cellular networks, base stations are categorized based on their ability to serve multiple User Equipment (UE) simultaneously, giving rise to SU-MIMO and MU-MIMO systems [9]. In SU-MIMO, the base station (BS) communicates with a single UE, transmitting one or more data streams using its antenna array. In contrast, MU-MIMO systems harness the power of BS antenna arrays to simultaneously broadcast multiple data streams to different UEs in distinct beams, sharing the same frequency resource without interference. mMIMO, a cutting-edge advancement of MIMO technology, leverages MU-MIMO principles to significantly enhance network capacity and user experience [10].

Recent research has delved into the downlink performance of MU-MIMO systems in 5G networks [11]. On this premise, this study focuses on improving downlink performance by analyzing MU-MIMO data transmission [12]. The categorization of user UE reception behavior based on inter-beam interference and the number of interference beams received is employed to achieve this improvement. Additionally, the network architecture is considered, and different scenarios within a specific time frame similar to the work of [13] are taken into account. These scenarios are influenced by users' mobility or stationariness relative to their sending and receiving devices. Although, several researcher have employed several systems to improve the downlink MU-MIMO systems, most of them are computationally complex. This complexity arises from the necessity of incorporating real-world factors such as interference, outages, consumption of energy, security, link reliability, and capacity limitations. Some of these factors stem from the shared utilization of the same frequency band by diverse technologies, including Bluetooth, Zigbee, and other WLAN systems [14]. To address these complexities, many studies have opted to trade-off computational complexity for in-depth analysis [10], [12], [15], or simplified factors like UE mobility to reduce complexity and focus on downlink Mu-MIMO [7]. To effectively serve the maximum number of UEs while considering their demands, locations, and mobility conditions, it is crucial to evaluate the available bandwidth, potential interference, and outage probability. This research, therefore, focuses on improving a downlink MU-MIMO technique for 5G networks that accounts for outage odds, enhances spectral efficiency, and strengthens link reliability. The rest of the paper discusses the followings: section 2 discusses literature that are related to the study. Section 3 delineates the methodology adopted in carrying out this research. Section 4 discusses the results obtained utilizing the ID-MU-MIMO algorithm. Section 5 concludes this paper.

II. Related Literature

This section reviews a few studies that have been shown to be helpful in enhancing Mu-MIMO's spectrum efficiency. Additionally, a summary of the methods employed by the assessed works to increase spectral efficiency, with a particular emphasis on Mu-MIMO outage mitigation, is discussed. With the knowledge gained from these works, this research was able to model an effective mechanism for MU-MIMO wireless communication system to limit outages in 5G and beyond wireless communications.

The energy efficiency of mmWave large MIMO systems was demonstrated through authors [4] evaluation of achievable sum-rate. Compared to traditional digital precoding techniques that assume a dedicated RF chain for each antenna and employ streamlined beamforming algorithms like ZF and MRC, mmWave large MIMO systems exhibited significant sum-rate and power reductions. The extended SOMP algorithm was proposed as a practical solution for hybrid precoding optimization, and its performance was shown to be near-optimal compared to standard MIMO. Massive MIMO technology has been found to significantly enhance system throughput when combined with basic signal processing techniques. The BER performance of SM and SSK schemes was analyzed, revealing that SM offers higher data rates but requires complex decoders and is more susceptible to errors, while SSK offers lower data rates but requires simpler decoders and exhibits lower BER. However, the impact of inter-beam interference was not considered in this study, which could potentially limit the effectiveness of strategies aimed at improving spectral efficiency.

The work of [15] explored the simultaneous alignment of Hermitian matrices representing desired signals and co-channel interference. Their approach simplified the analysis of critical performance measures like probability of outage, ergodic capacity, and spectral efficiency by leveraging joint unitary eigenvectors and their corresponding eigenvalues. These authors integrated digital baseband beamforming vectors into transmitter-side channel weight matrices, facilitating the representation of SINR in a standard quadratic form. Moreover, they devised a real scalar objective function to quantify the correlation loss linked with joint-diagonalization. Acknowledging the hardware limitations of mmWave systems, they employed baseband beamforming to optimize the objective function. The results delineated from the simulation showed that the proposed beamforming algorithm outperformed various nonlinear optimization methods in terms of time complexity and correlation assessment, surpassing, notably demonstrating efficiency in the "active-set" approach. While the targeted signal and co-channel interference were considered, inter-beam interference remained unaddressed. Moreover, the computational complexity was relatively substantial, potentially affecting the communication link's reliability.

The increasing number of transmit antennas and planned users on the same frequency response led to a significant rise in the computing complexity of outage probability and coverage probability calculations, as observed by [12]. To assess the coverage performance of downlink cellular MU-MIMO networks, the authors proposed combining exponential functions to approximate the complementary cumulative distribution function of received signal gain. Prony's technique was employed to simplify the calculation of expectations related to intra-cell and inter-cell interference. Simulation results based on this method indicated that downlink coverage probability remained unaffected by an increase in the number of base stations. While a key objective was to reduce the computational complexity of coverage probability determination, the method did not consider the SIR values of users connected to the same cell. These shortcomings are likely to hinder the method's performance in real-world scenarios.

Digital federated learning and over-the-air compression techniques were employed in [16] to enhance signal processing optimization. The authors formulated problems tailored to user demands while minimizing Mean Square Error (MSE) of parameter vectors. These problems were addressed using block coordinated descent-based iterative methods. Moreover, the authors optimized the precoding matrices of the over-the-air compression system. The proposed methodology demonstrated superior performance compared to the standalone digital federated learning scheme, particularly with increasing user participation. However, a drawback of this approach was its heightened computational complexity, which could potentially jeopardize the communication link's reliability.

To enhance spectral efficiency and communication link reliability in MU-MIMO for 5G and future wireless systems [7], a mechanism was developed. Despite user demands, the system was designed to handle MU-MIMO in downlink with multiple antenna users, delivering optimal QoS to all the devices that are connected. Three user allocation scenarios were considered: random, uniform, and default allocation for antennas serving multiple users. The uplink and downlink were influenced by the random demand on these scenarios. Throughput utilization, network capacity, data rate for each device and the network, distances between users and antennas and from other devices, path loss, channel gain, and interference were additional variables estimated to model these scenarios. The uniform allocation algorithm outperformed default and random allocation algorithms in most trials, surpassing all three scenarios. In other words, RB utilization and SINR were more effective with uniform allocation. The authors did not consider user mobility, which could negatively impact communication link reliability in real-world scenarios.

In their work [11], the authors introduced an innovative, low-complexity approach combining multi-beamforming and Maximal Likelihood-Multi-User Detection (ML-MUD). They utilized a Radix Factorization-based FFT (RF-FFT) and integrated sub-detector systems to significantly reduce complexity without compromising error rate performance. The proposed architecture, known as RF-FFT - Multi-Beamforming (RF-FFT-MBF), holds immense promise in mitigating hardware complexity, energy consumption, and fulfil the throughput needs of 5G devices. To showcase the efficiency of the scaled ML-sub detector system on the downlink, simulation results of this detector were compared against conventional ML detectors. The outcomes delineated that the proposed detector outperformed the conventional ML detectors in terms of hardware and energy efficiency, boasting minimal performance.

Extensive research on downlink MU-MIMO systems has predominantly focused on ad hoc network topologies, with limited attention given to cellular networks and UE mobility. While some studies have explored cellular networks, they either disregard UE mobility or employ computationally demanding approaches. Despite significant efforts to address interference, throughput, SINR, outage probability, spectral efficiency, and link communication reliability, challenges like interference and high computational complexity persist. This research presents an improved MU-MIMO Downlink mechanism for 5G and beyond wireless cellular networks, leveraging on the work of [12]. The proposed mechanism is expected to enhance spectral efficiency, link communication reliability, as well as reduce the probability of outage in comparison to existing systems. Section 3 outlines the methods and system model designed to achieve these goals.

III. Methodology

The development process for the Improved Downlink MU-MIMO Downlink (ID-MU-MIMO) scheme is described in this section. The methods used for developing the system model for the ID-MU-MIMO algorithm are explained in subsections I to V.

I. ID-MU-MIMO Algorithm

Building upon the foundations established in [7] and [12], this work adopts a hybrid approach that merges techniques from both works to address the limitations of [7], namely its overlook for UE mobility, while simultaneously reducing computational complexity. The proposed ID-MU-MIMO algorithm is the culmination of these considerations. To achieve these objectives, this work expands the network scenarios for UEs beyond those presented in [7] by introducing two additional network case scenarios, which are represented in the steps outlined below.

II. Defining the Mobile and Stationary Events of UEs at the Start of Each Time Frame

In a real-world setting, it is assumed that UE distribution throughout a coverage region is random. Inter-beam interference and the quantity of received interference in a MU-MIMO broadcast are both impacted by the mobility status of the UEs within the coverage area. According to published findings, measuring the state of a channel continuously would probably be computationally challenging because the channel's state, the power delivered, etc., are all dynamic. As such, the data transfer to UEs is taken into account within a time frame to reduce this complexity. It is assumed, based on the literature, that the channel's condition and transmitted power will remain constant over this time. In this work, certain premises are adopted. It is simpler to look into co-channel and inter-beam interference at this specific time. A closed form outage probability assessment of an instantaneous MU-MIMO transmission is also permitted by this consideration. In light of the aforementioned, this work considers the placement of UEs in a coverage area to be randomly allocated according to Spatial Poisson Point Process (SPPP) with intensity $(\varkappa)$. The set of BS are represented as $\mathrm{S}(\varkappa) = \{\mathrm{B_i}\}$, where $\mathrm{B_i}$ is the position of the BS, at an instant in time, *i*.

The received signal of the receiving UE, k, in the MU-MIMO data transmission phase is mathematically stated as follows [14, 17]:

$$y_k = \sqrt{\frac{P_t}{k} D_k^{-\beta}} h_k^H w_k s_k + \sum_{j \in K, j \neq k} \sqrt{\frac{P_t}{k} D_k^{-\beta}} h_k^H w_j s_j + \sum_{\tau \in \phi / T_k} \sqrt{P_t \left| Z_\tau \right|^{-\beta}} g_{\tau K^s \tau} + \eta_k \tag{1}$$

Where y_k represents the received signal by UE, *k*, P_t denotes the power transmitted by *k*, T_k denotes the BS, $\boldsymbol{h}_k \epsilon \mathbb{C}^{N_t \times 1}$ represents the channel gain vector between the k and T_k, $\boldsymbol{g}_{\tau,k} \epsilon \mathbb{C}^{1\times 1}$ represents the channel gain vector between the k and τ, $\boldsymbol{S}_k \epsilon \mathbb{C}^{K\times 1}$ signifies the transmitted symbol from the BS, n_k denotes the AWGN with zero mean and variance of σ^2, $\sqrt{\frac{P_t}{K} D_k^{-\beta}} \boldsymbol{h}_k^H \boldsymbol{w}_k \boldsymbol{s}_k$ denotes the desired signal, $\sum_{j\epsilon K, j\neq k} \sqrt{\frac{P_t}{K} D_k^{-\beta}} h_k^H \boldsymbol{w}_j \boldsymbol{s}_j$ denotes the inter-beam interference signal, $\sum_{\tau\epsilon\Phi/T_k} \sqrt{P_t |Z_\tau|^{-\beta}} g_{\tau k^{s_\tau}}$ depicts the co-channel interference signal.

The presence or absence of inter-beam interference for a receiving UE, k, is subject to the variations, that is, the change or stationariness the channels of the wireless experiences with respect to the location of the BS during the time period. In the case of stationary UEs, the orthogonality of the beams ensures the elimination of inter-beam interference. However, for moving UEs, their own beams interfere with other beams, and the beams of stationary UEs interfere with the beams of moving UEs. To evaluate the performance of MU-MIMO transmission, we characterize the UE behaviour based on the occurrence and intensity of inter-beam interference. By defining a set of events that represent different UE behaviours, we simplify calculations and gain insight into the impact of inter-beam interference on MU-MIMO performance. The beam of a motionless UE interferes with the beams for M moving UEs when the event $\mathcal{H}_2$ with $0<M<K$ occurs, but the beam of a moving UE interferes with the beams for K-1 UEs. In light of this, the

proposed measurement of the instantaneous received SINR for stationary and moving UEs is denoted as event $\mathcal{H}_2^s$ and $\mathcal{H}_2^m$, respectively [12].

Case One

In this case, which is referred to as $\mathcal{H}_1$ both the UEs in the MIMO system are stationary during the considered time frame.

Case Two

Event $\mathcal{H}_2$ refers to a circumstance in which the UEs are mobile within the time period. For this event $M(1 < M \leq K)$. Since a mobile user was present at every time point in the study period, $M \geq 0$ in this instance. The probability that the instantaneous received SINR falls below the required SINR threshold is called the outage probability of a MU-MIMO transmission. The predicted probability of outage is given as in (2) as delineated in the work of [12].

$$P_k^{\exp}(\xi_{thres}) = \sum_{i=1}^{3} \wp(H_i)\wp(\xi_{k,\xi_i}^{ins} \leq \xi_{thre}) = \sum_{i=1}^{2} \wp(H_i)\wp(\xi_{k,\xi_i}^{ins} \leq \xi_{thres}) + \left[\wp(H_3)\times\left[\wp(H_3^S)\wp(\xi_{K,H_3^S}^{ins} \leq \xi_{thres}) + \wp(H_3^m)\wp(\xi_{K,H_3^m}^{ins} \leq \xi_{thres})\right]\right] \tag{2}$$

where $\wp(\mathcal{H}_\text{i})$ denotes the likelihood of the event $\mathcal{H}_\text{i}$ occurring and $\xi_{k,\mathcal{H}_i^s}^{ins}$ signifies the instantaneous SINR received by k at the time of the event $\mathcal{H}_\text{i}$. However, an event when both the UE and the BS station are mobile is not taken into account in this work's total of the outage probability weighted by the likelihood of defined occurrences. As a result, only a total of $\mathcal{H}_2$ events, as identified in cases one and two, can be accommodated by the probability of weighted events $\mathcal{H}_\text{i}$, which is decreased (i-1) as a result. The requirements as they apply to scenario one take into account the likelihood that the UE and the gNB are stationary, and as a result M=0. The second event, on the other hand, takes into account a scenario in which the UE is mobile and the gNB is stationary. In this case, $M \geq 0$ since a UE is always mobile at any point in the time fame considered.

When the two aforementioned events are taken into account and applied to the system chosen for this study, the events reduce from $\mathcal{H}_3$ to $\mathcal{H}_2$, and the influence on the outage probability sum multiplied by the probabilities of the defined events in (2) results in (3).

$$P_k^{\exp}(\xi_{thres}) = \sum_{i=1}^{2} \wp(H_i)\wp(\xi_{k,\xi_i}^{ins} \leq \xi_{thre}) = \wp(H_i)\wp(\xi_{K,\xi_{thres}}^{ins})\times \left[\wp(H_2)\wp(\xi_{K,H_2^S}^{ins} \leq \xi_{thres}) + \wp(H_2^m)\wp(\xi_{K,H_2^m}^{ins} \leq \xi_{thres})\right] \tag{3}$$

The implications of the lower weighted sum affect both the performance factors that are examined and the probability of events.

III. System Model

To model the occurrences $\mathcal{H}_1$ and H_2^M, it is crucial for this study to first replicate the MD-MU-MIMO scheme model before modifying it to take the mobility of the UEs into account. When taking into account the UEs' mobility, care must be given to elements that could raise the likelihood that a UE would suffer a loss of signal quality or be unable to establish a trustworthy connection because of elements like interference, fading, and channel circumstances. The term "outage probability" is used to describe this likelihood. When simulating the MD-MU-MIMO scheme, it is crucial to keep in mind that Mu-MIMO gives a great capacity boost by utilizing multiple antennas and supporting single-antenna users without the need to increase network bandwidth. Literature studied earlier reveal that the integration of multiple antennas at the communication terminals significantly enhances the communication system's spectral efficiency and ensures a more reliable communication link. A MIMO system typically uses several broadcast and receive antennas. Each antenna, while intended to receive specific components of the signal, also captures indirect components intended for other antennas on the same channel. To maximize system performance, data intended for transmission is divided into separate, independent data streams, a number that is typically equal to or less than the number of available antennas. This design results in a linear increase in system capacity as the number of flows grows, aligning with the principles described in the Shannon-Hartley theorem for MIMO, denoted as (4) [7].

$$C \leq MB \log_2\left(1+\frac{S}{N}\right) \quad (4)$$

where C is the channel capacity in bps, B is the bandwidth in Hz, S is the average received signal power in Watts, and N is the average power of the noise in Watts. The maximum feasible data rate of a system is obtained by multiplying the number of pulse levels (M) by the system bandwidth and the base 2 logarithm of the SNR + 1 [7].

$$MaxDR = B \log_2\left(1+\frac{S}{N}\right) \quad (5)$$

In contrast, the Maximum Data Rate (MaxDR) rises roughly linearly when the SNR is low. Although, simply aiming for a high SNR is not very effective; a better strategy involves dividing the SNR throughout the streams, which multiplies the maximum data rate that can be transmitted. One method to achieve this distribution is through spread spectrum techniques like Code Division Multiple Access (CDMA), which spread the signal over a broader bandwidth. MU-MIMO technology enhances system capacity and communication reliability. MU-MIMO is particularly advantageous for the uplink since UE employs just a single antenna for transmission, reducing complexity. This work aims to leverage multiple antennas at both the user and base station (BS) ends of the communication link to enhance the achievable spectral efficiency and overall reliability of the communication system and link. Spectral efficiency (SE) refers to the total amount of data transmissions that can occur over a given bandwidth within a cell of a cellular network. The cell throughput, expressed in bit/s/Hz, is obtained by multiplying the SE by the bandwidth. Since the bandwidth is fixed, increasing cell throughput is the preferable solution. For the system to simultaneously support the maximum number of UEs within a cell while maintaining the same bandwidth, it is crucial to achieve higher spectral efficiency. The spectral efficiency of 5G New Radio (NR) (bits/sec/Hz) can be approximated as follows [7]:

$$SE = \frac{Throughput\,(bps)}{Channel\ Bandwidth\,(Hz)} \quad (6)$$

It is essential to follow the 3GPP standard suggestion in order to get accurate results from the computed spectral efficiency in a network. This involves doing an extensive throughput calculation that takes into account a variety of factors, including the bandwidth, number of MIMO layers, modulation type, and frequency range. Only one aggregated component carrier is required in order to guarantee reliable results. Following that, the channel bandwidth must be divided by the throughput. A variable number of users are served by 25 antennas that make up the ID-MU-MIMO architecture. The 5G NR Frequency Radio 2 (FR2) type's user count varies depending on the deployment environment. As a result of the proposed topology's consideration of both micro cells and metro cells, micro cells can accommodate a maximum of 256 users, whilst metro cells can accommodate more than 250 people. The objective of this ID-MU-MIMO technique is to determine the optimal number of UEs that should be scheduled and served per cell within the network to maximize spectral efficiency. However, multi-cell systems create difficulties that require a variety of criteria and parameters for validation of results. The simulation takes into account several different variables, including pilot allocation, hardware, hardware configuration, and block lengths. In the simulated network design, the UL and DL transmission modes have a substantial impact on UE performance.

In an MU-MIMO system, UE equipped with M_a single antennas is connected to the BS using N antennas during the downlink. Different processing strategies are taken into consideration, including Zero-Forcing (ZF), Maximum Ratio (MR) combining/transmission, and full-Pilot ZF (P-ZF) strategy. In a fully distributed coordinated beamforming system, the P-ZF actively suppresses inter-cell interference. The usage of the same matrix for scheduled users who are in the waiting list is made possible by the assumption that each scheduled user's precoding matrix is almost similar. Additionally, every UE engages in single-user identification, and its bit rate is determined by its bandwidth and Signal-to-Noise Ratio (SNR), where f_l is essentially a function that characterizes the performance of the link [7].

$$R_b = B \times F_l(SNR) \tag{7}$$

This work addresses the complexities of multi-cell systems and considers various features and processing algorithms in the simulated network topology, with the ultimate goal of optimizing network performance. The SINR(x) function allows the definition of SINR based on the user's location. Spectral efficiency at a UE location is determined by the relationship between the bit rate and the user bandwidth at that location. Each BS serving a cell allocates subcarriers of the total bandwidth to individual users based on the methodology described above. This assignment ensures that different users within the same cell, served by the same BS, receive different subsets of subcarriers. Consequently, since each BS transmits at a constant power, users within the cell experience interference from their respective base stations.

Modifying the above equations to consider events ($\mathcal{H}_2^M$) that take into account the mobility of the UEs

$$C \leq M_a B \ \log_2\left(1 + \xi_{k,\mathcal{H}_2^m}^{ins}\right) \tag{8}$$

where $\xi_{k,\mathcal{H}_2^m}^{ins}$ is defined as Eq. 8

$$\xi_{k,\mathcal{H}_2^m}^{ins} = \frac{P_t/KD_k^{-\beta}\left|\boldsymbol{h}_k^H\boldsymbol{w}_k\right|^2}{\sigma^2+\phi\sum_{j\epsilon U}(P_t/K)D_k^{-\beta}\left|\boldsymbol{h}_k^H\boldsymbol{w}_j\right|^2+\sum_{\tau\epsilon\Phi/T_k}P_t|Z_\tau|^{-\beta}\left|g_{\varphi,k}\right|^2} \tag{9}$$

where $P_t/K\,D_k^{-\beta}$ represents desired signal power, $|\boldsymbol{h}_k^H\boldsymbol{w}_k|^2$ denotes the squared magnitude of the channel coefficient between the transmitter and the intended receiver, multiplied by the squared magnitude of the weight vector for the intended user, σ^2 represents noise power, $\phi\sum_{j\epsilon U}(P_t/K)D_k^{-\beta}\left|\boldsymbol{h}_k^H\boldsymbol{w}_j\right|^2$ represents the interference caused by other users in the system, and $\sum_{\tau\epsilon\Phi/T_k}P_t|Z_\tau|^{-\beta}\left|g_{\varphi,k}\right|^2$ represents the interference caused by other cells in the system, particularly focusing on the antennas in those cells that interfere with the intended receiver.

As such, the MaxDR computed is defined as in Eq. 10

$$MaxDR = B \ \log_2\left(1 + \xi_{k,\mathcal{H}_2^m}^{ins}\right) \tag{10}$$

Furthermore, the definition of spectral efficiency (SE) is as follows:

$$SE = \frac{iTh_{tot}^{\exp}}{Channel\ Bandwidth\,(Hz)} \tag{11}$$

Since the proposed expected throughput $\left(iTh_{tot}^{\exp}\right)$ proposed is denoted in Eq. 12 as:

$$iThr_{tot}^{exp} = \sum_{k=1}^{K}\left(\wp(\mathcal{H}_1)Thr_{k,\mathcal{H}_1}^{exp} + \wp(\mathcal{H}_2)\left(\wp(\mathcal{H}_2^{s})Thr_{k,\mathcal{H}_2^{s}}^{exp} + \wp(\mathcal{H}_2^{m})Thr_{k,\mathcal{H}_2^{s}}^{exp}\right)\right) \tag{12}$$

As such, substituting (12) into (11) yields:

$$SE = \frac{\sum_{k=1}^{K}\left(\wp\left(\mathcal{H}_1\right)Thr_{k,\mathcal{H}_1}^{\exp} + \wp\left(\mathcal{H}_2\right)\left(\wp\left(\mathcal{H}_2^{s}\right)Thr_{k,\mathcal{H}_2^{s}}^{\exp} + \wp\left(\mathcal{H}_2^{m}\right)Thr_{k,\mathcal{H}_2^{m}}^{\exp}\right)\right)}{Channel\ Bandwidth\left(Hz\right)} \tag{13}$$

While the resource block usage is given in Eq. 14 as:

$$R_b = B \times F_l\left(\xi_{k,\mathcal{H}_2^{m}}^{ins}\right) \tag{14}$$

Equation (8) to (14) form some of the fundamental algorithms used to model the ID-MU-MIMO algorithm.

Equation (15) provides the estimated probability of outage for the instantaneous MU-MIMO transmission. The average of the outage probabilities for the cases of the UEs' events is known as the expected outage probability.

$$P_k^{\exp}(\xi_{thres}) = \sum_{i=1}^{2}\wp(H_i)\wp(\xi_{k,\xi_i}^{ins} \le \xi_{thre}) = \wp(H_i)\wp(\xi_{K,\xi_{thres}}^{ins})\times \left[\wp(H_2)\wp(\xi_{K,H_2^{S}}^{ins} \le \xi_{thres}) + \wp(H_2^{m})\wp(\xi_{K,H_2^{m}}^{ins} \le \xi_{thres})\right] \tag{15}$$

Where $P_k^{exp}(\xi_{thres})$ is the outage probability (P_{outage}) based on a given threshold (ξ_{thres}), $\wp(\mathcal{H}_\mathrm{i})$ represents the probability of event $\mathcal{H}_\mathrm{i}$ given as $P(M)$ and $\xi_{k,\mathcal{H}_i^{s}}^{ins}$ depicts the instantaneous received SINR of the receiving node (k) when the event $\mathcal{H}_\mathrm{i}$ occurs given as $P((SINR < \xi_{thres}) \mid M)$.

The ramifications of the reduced weighted sum impact the probability of events and the performance factors measured. Outage probability represents the probability that a wireless communication link will fail due to various factors, including interference and signal quality. Equations (16) and (17) evaluate the PDF on event $\mathcal{H}_i$ using equations (16) and (17).

$$\wp\left(\mathcal{H}_1\right) = \left(P_{state}e^{-\theta T_{frame}}\right)^{K+1} \tag{16}$$

Where $\wp(\mathcal{H}_1)$ represents the outage for $\mathcal{H}_1$, P_{state} is a parameter denoting the probability that a specific state (e.g., a certain channel state or interference level) occurs during the communication. $e^{-\theta T_{frame}}$ denotes the exponential function where T_{frame} represents the duration of time for which the communication is observed. And $K+1$ is the exponent that models the outage probability for K+1 receiving users.

$$\wp(\mathcal{H}_2) = \left(P_{state} e^{-\theta T_{frame}}\right)^{K-M+1} \left(1 - P_{state} e^{-\theta T_{frame}}\right)^{M} \tag{17}$$

Equation (17) models the outage probability for a more complex scenario where there are K+1 users in the MU-MIMO system, and it depends on the probability of a specific state (P_{state}), the time duration (T_{frame}), the number of users (K+1), and the Mobile UEs. These equations are crucial for assessing the system's performance and understanding the probability of outage in complex wireless scenarios.

These equations are the equations for the PDFs on event $\mathcal{H}_i$. The PDFs are the probabilities that the UEs are in good or bad channel condition, given that the UEs are in event $\mathcal{H}_i$. The outage probability of instantaneous MU-MIMO transmission using the appropriate equation, depending on the value of ϕ. If ϕ = 0, then the outage probability is obtained using equations (18).

$$P_k^{ins}(\xi_{thres}) = 1 - \sum_{m=0}^{N_t-K} \frac{(-\omega)^m}{m!} \frac{(d)^m}{d\omega^m} \mathcal{L}_{I_{K,CCI(\omega)}} \tag{18}$$

Where $\mathcal{L}_{\rho I_{k,IBI}}(\omega)$ signifies the Laplace transform of the interference seen by user K due to Inter Block Interference (IBI), scaled by ρ. Equation (16) combines both IBI and ICI to compute the outage probability for ξ_{thres}. It quantified the probability that ξ_{thres} experiences by the *k-th* user when it falls below the defined ξ_{thres} due to interference.

To enhance the pragmatism of the simulation studies, additional complex channel models that account for realistic propagation conditions, including Non-Line-of-Sight (NLOS) components and variable mobility patterns were considered by further modifying the Laplace transforms $\mathcal{L}_{\rho I_{k,IBI}}(\omega)$ and $\mathcal{L}_{I_{k,CCI}}(\omega)$. As such, the parameter ρ_{NLOS} was introduced to capture the effects of NLOS components and $f_{mobility}(t)$ was introduced to represent the mobility patterns of users over time (t). Hence, the redefined Laplace are:

$$\mathcal{L}_{\rho LOS\, I_{K,IBI}}(\omega) = \mathcal{L}\left\{\rho LOS . I_{K,IBI}(t)\right\} \tag{19}$$

$$\mathcal{L}_{K,CCI}(\omega, t) = \mathcal{L}\left\{I_{K,CCI}(t) . f_{mobility}(t)\right\} \tag{20}$$

Hence, equation (18) is redefined as:

$$P_k^{ins}(\xi_{thres}) = 1 - \sum_{m=0}^{N_t-K} \frac{(-\omega)^m}{m!} \frac{(d)^m}{d\omega^m} \mathcal{L}\left\{\rho NLOS . I_{K,IBI}(t)\right\} . \mathcal{L}\left\{I_{K,CCI}(t) . f_{mobility}(t)\right\} \tag{21}$$

IV. Algorithm of the ID-MU-MIMO Scheme

The ID-MU-MIMO algorithm is defined in Algorithm 1. The network design in the algorithm takes into account the mobility states of the user equipment. The MU-MIMO system's overall performance in a realistic environmental context is significantly influenced by the movement of the user equipment. Consequently, the suggested network model regards UEs as being distributed at random over the BS's coverage area. Both of the ID-MU-MIMO algorithm's cases are delineated in Algorithm 1. The first event denoted as $\mathcal{H}_1$ indicates that the UEs are immobile at the start of a set time frame and do not move during the duration not less than T_{Frame}. The second scenario, $\mathcal{H}_2$

considers the movement of the UE during T_{Frame}. The input parameters required to simulate and model the network topology of the wireless cellular network encompass the variables associated with mobility events. In the case of UEs linked to the gNB, the work assesses the mobility state of these events prior to calculating the resource block of each user. Concerning the two states, the resources are computed for one in which the effects of interference are removed, that is, where $\phi = 0$ and another in which the interference is considered, that is, $\phi = 1$. Whether inter-beam interference is taken into account or not, the goal of this modification is to reduce processing time. An outage in the network would be less likely using the suggested ID-MU-MIMO mechanism.

Algorithm 1 ID-MU-MIMO algorithm

Input $\mathcal{H}_i$, T_{Frame}, i, $\mathcal{H}_2^s$ *and* $\mathcal{H}_2^m$
Input Modulation type, bandwidth, Number of MIMO layers, Bandwidth, frequency range
Output Outage probabilities, spectral efficiency

For spatial distribution of users at time instant, U_i in the simulated network topology are uniformly or randomly distributed
  For each U_i
    If i is connected
      For each U_i trying to connect
        Utilizing Eq. (6) and Eq. (12), determine the maximum data rate the UE is capable of achieving
        i ++
      End for
    Else
      i ++
      Evaluate the expected outage probability using equation Eq. (3)
      Compute PDF on events $\mathcal{H}_i$
    If $\phi = 0$
      Compute outage probability
      Determine the RB's for each user using Eq. (6)
    Else
    If $\phi = 1$ and 0 < M < K
      Compute outage probability
      Compute each user's RB using Eq. (12)
    End if
    End if
   End if
End for
For each cell topology
  Calculate BSs power allocated to the connected users
  Contrast performance with existing approach
  K++
  End for
End for

V. Simulation Parameters

The simulation parameters adopted for the ID-MU-MIMO mechanism are presented in Table 1. These values are used to evaluate the performance of the conventional IEEE 802.11ax approach, the mechanism for downlink MU-MIMO, and the modified ID-MU-MIMO mechanism adopted in this research.

Table 1: *Extracted Parameters* [7, 12]

Parameters	Values
Bandwidth, B	160MHz
Capacity speed, V_c	3.39 Gb/s
Carrier bandwidth, B_c	400MHz
Downlink rates	20Gbps
Link rate	867Mbps
Path loss exponent	4
Mobile receiving nodes	1, K/2, K
Receiver noise power	-32dBm
Resource block frames, DL	275
Resource block frames, UL	275
Number of discrete rates	4
Average time interval	1s
Scenario	4 antennas AP
SINR threshold	-30dB
Sub Carrier Spacing	120KHz
Users for each scenarios	200, 250, 300
Distance between Tx and Rx, R_x	100m

IV. Results and Discussion

A thorough overview of the study's results is provided in this section by the presenting findings and their impacts.

I. Interference vs Users

Figure 1 represents the effect of interference as it affects the performance of the UEs in the MU-MIMO system. The events considered to weigh the impact are $\mathrm{H}_1 = 1 - (M/K)$ and H_2^M at $M(0 < M < K)$ where H_1 represents the event where the UEs are stationary and H_2^M represents the events where some or all of the receiving UEs (K) are mobile. The impact of this event as applied in the developed scheme, the IEEE 802.11ax scheme, the random MD-MU-MIMO scheme and the uniform MD-MU-MIMO scheme are represented in Figure 1. In all schemes, both the BS and UEs deployed are considered to be stationary. For the receiving UEs, inter-beam interference is present or absent depending on whether the wireless channel changes with the UE's locations overs the predetermined time period. Orthogonality of beams and the elimination of inter-beam interference are both possible because all nodes are kept fixed throughput the time period. Since the ID-MU-MIMO algorithm takes the mobility of the UEs into consideration, it examines the event H_2^M where some nodes can be fixed and others mobile. Here, 0<M<K is appropriate. Therefore, K-1 UEs in the system could cause inter-beam interference with mobile UE (M). For both IEEE 802.11ax and the MD-MU-MIMO system, user deployment of 200, 250, and 300 are taken into account consistently. For the ID-MU-MIMO algorithm, the UEs are randomly deployed and this is also considered for one of the deployment scenarios for the MD-MU-MIMO scheme.

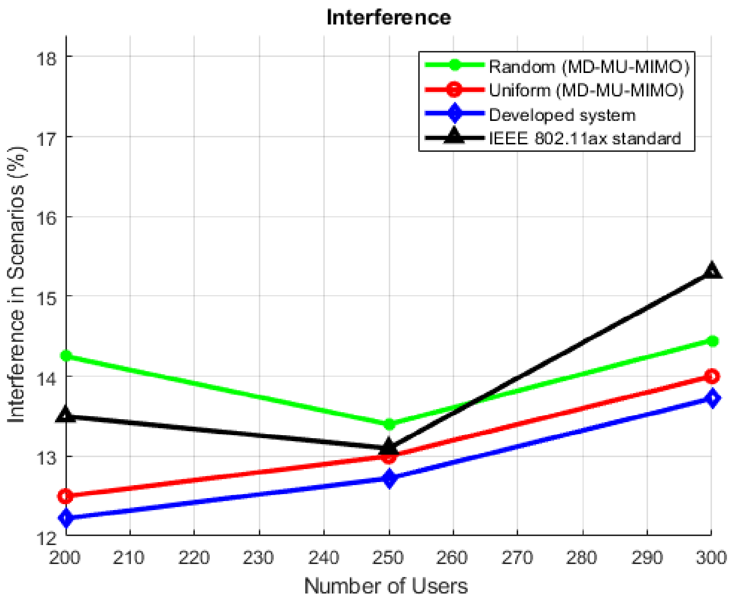

Figure 1: *Interference vs Users*

The performance of the designed ID-MU-MIMO scheme is shown in Figure 1, and it takes into account the aforementioned deployment situations as well as the UEs' mobility in order to model the system to actual environmental settings. The IEEE802.11ax algorithm and the existing MD-MU-MIMO algorithm did not take the UE's mobility into account. Figure 1 shows that, for the existing random MD-MU-MIMO algorithm, interference values decreased from 14.4% to 13.5% between the use cases distributions of users from 200 to 250, and for the IEEE 802.11ax values, interference values decreased from 13.5% to 13.1%. The source of this behaviour is a change in the measured distances between users placed in the network due to the random spatial deployment of users. As a result, there will inevitably be fluctuating channel conditions that could either raise or decrease interference for network users, as evidenced by the work's random reduction of interference. However, it is typically noted that when the number of users deployed in the system increases, interference of the system within the provided time frame generally increases for the system. In comparison to the IEEE 802.11ax protocol, the percentage gains in interference for the random and uniform distributions of users, respectively, were found to be 4.98% and 5.55% from the results obtained per use case scenario taken into account for the users. Additionally, comparing the ID-MU-MIMO method to the IEEE 802.11ax scheme, interference was also improved by 7.71%. The percentage reductions obtained for the designed and existing schemes both demonstrated that they outperform the current IEEE 802.11ax system. When compared to the results of the random and uniform MD-MU-MIMO algorithms, the created ID-MU-MIMO scheme demonstrated interference reduction in percentages of 8.90% and 2.28%, respectively.

II. SINR vs Users

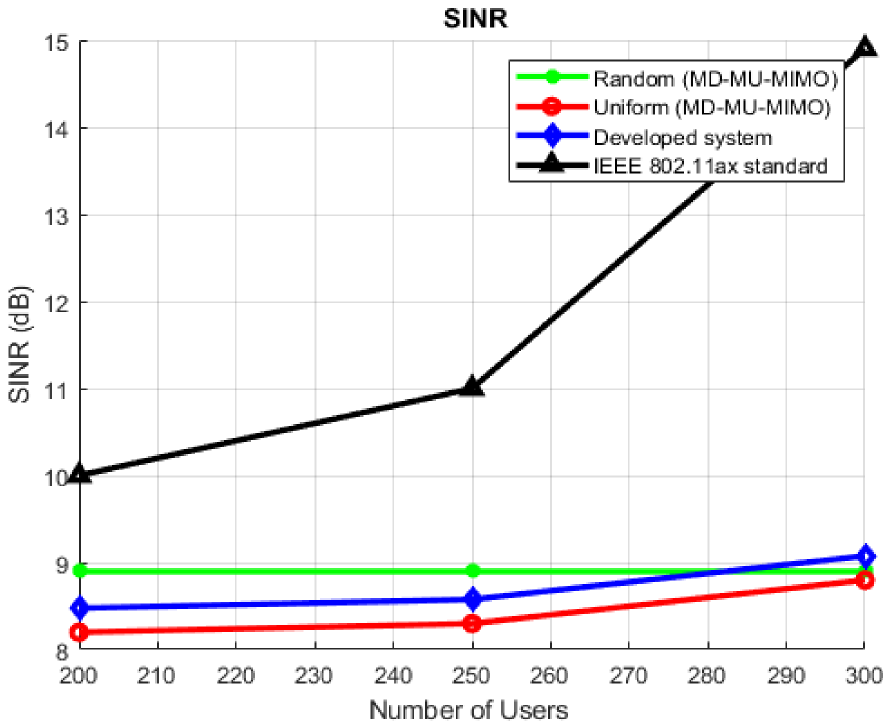

Figure 2: *SINR vs Users*

In maintaining the conditions for H_1 and H_2^m, Figure 2, illustrates the change in SINR, which revealed a considerable increase in SINR percentages from 11.0% to 14.9% in the IEEE 802.11ax values between the use case distributions of users from 200 to 250. This is probably caused by the low SINR. As a result, the maximum data rate rises approximately linearly. However, focusing just on high SINR percentages is ineffective because there is a greater likelihood of signal overlap and interference when more users broadcast at the same time while using the same time and frequency resources. Additionally, it was found that the performance of the random user deployment over a rising user count remained steady in this iteration of the SINR performance for the MD-MU-MIMO scheme. The interference as seen in this iteration of the simulation is probably low relative to the noise, which is the likely explanation for this stability as the focus is on the receiving UEs rather than the transmitting BS. As a result, the noise power and channel gain, which are unaffected by the user count, dictate the SINR. In comparison to the IEEE 802.11ax method, percentage gains in SINR of 23.45% and 27.43% for the random and uniform distribution of users, respectively, were seen from the findings produced per use case scenario taken into account for the users. Additionally, as compared to the IEEE 802.11ax system, the ID-MU-MIMO technique demonstrated a SINR improvement of 22.55%. The percentage reductions obtained for the designed and existing schemes both demonstrated that they outperform the current IEEE 802.11ax system. When the performance of the new ID-MU-MIMO scheme was compared to that of the random and uniform MD-MU-MIMO algorithms, the SINR was reduced by percentages of 4.27% and 2.75%, respectively.

III. Resource Block Usage vs Users

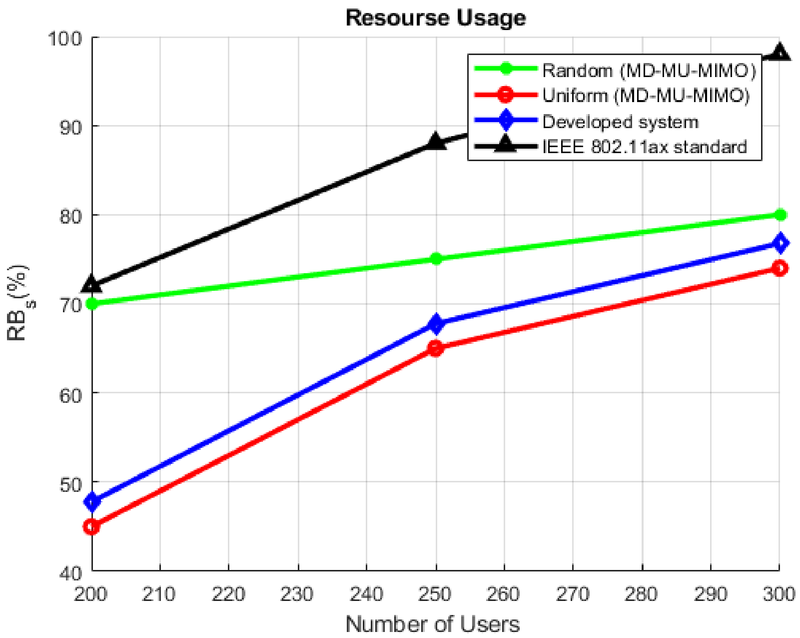

Figure 3: *Resource Block Usage vs Users*

In Figure 3, the results obtained per use case scenario considered for users, percentage improvements of 11.65% and 28.63% were observed in the use of resource blocks for random and uniform distribution of users respectively, compared to the IEEE 802.11ax scheme. Furthermore, the ID-MU-MIMO scheme showed a 25.87% improvement in interference compared to the IEEE 802.11ax scheme. The percentage reduction obtained from the existing and developed scheme showed that both improve over the existing IEEE 802.11ax scheme. The developed ID-MU-MIMO scheme showed a reduction in resource usage of 20.05% and 3.89% compared to the performance of the random and uniform MD-MU-MIMO algorithm, respectively.

V. Conclusion

Using a closed-form outage probability of a discrete time frame of MU-MIMO transmission, this work presented an effective mechanism for downlink MU-MIMO for 5G networks. This work examined the interference, SINR, and resource block usage over a specified time period, the outage probability of the receiving UEs in a specified area, and spectral efficiency in a modified MU-MIMO system to confirm the model's performance. The outcomes showed that the proposed ID-MU-MIMO scheme outperforms both the IEEE 802.11ax standard and current MD-MU-MIMO systems. In particular, compared to IEEE 802.11ax, the ID-MU-MIMO technique achieved a 7.71% reduction in interference. When compared to the performance of the random and uniform MD-MU-MIMO algorithms, the proposed ID-MU-MIMO scheme showed a reduction in interference in percentages of 8.90% and 2.28%, respectively. The ID-MU-MIMO scheme outpermed the random and uniform MD-MU-MIMO algorithms in terms of SINR, outperforming them by 4.27% and 2.75%, respectively, and resource block use, outperforming them by 20.05% and 3.89%, respectively. Future work is recommended to examine how a use case scenario of increasing the number of receiving UEs (K) can impact the probability of outage over a defined time frame and over a defined area, as well as determining the spectral efficiency under the conditions considered for a higher number of receiving UEs. Additionally, Machine Learning (ML) approaches can be adopted to modify the ID-MU-MIMO algorithm to dynamically adjust to varying network conditions and UE densities in real time to maximize performance under varying conditions.

References

[1] Struzak, R. Tjelta, T. and Borrego, J. P. (2015). On Radio-frequency Spectrum Management. *URSI Radio Science Bulletin*, 354: 11-35.

[2] Dala, P. S. V. Dester, P. S. Soares, P. F. M. Gomes Silva, D. and De Figueiredo, F. A. P. Tejerina, G. R. L. ... and Cardieri, P. (2023). Emerging MIMO Technologies for 6G Networks. *Sensors*, 23, 4: 1-20.

[3] Wong, V. W., Schober, R. and Ng, D. W. K. (Eds.). (2017). *Key technologies for 5G wireless systems*. Cambridge university press.

[4] Nalband, A. H., Sarvagya, M. and Ahmed, M. R. (2020). Optimal hybrid precoding for millimeter wave massive MIMO systems. *Procedia Computer Science*, *171*: 810-819.

[5] Singh, J. and Kedia, D. (2020). Performance improvement in large-scale MU-MIMO system with multiple antennas on user side in a single-cell downlink system. *Arabian Journal for Science and Engineering*, *45*(8): 6769-6789.

[6] Akpakwu, G. A., Silva, B. J., Hancke, G. P. and Abu-Mahfouz, A. M. (2017). A survey on 5G networks for the Internet of Things: Communication technologies and challenges. *IEEE access*, *6*, 3619-3647.

[7] Barri, E., Bouras, C., Kokkinos, V. and Koukouvela, A. (2021). A Mechanism for Improving the Spectral Efficiency in mu-MIMO for 5G and Beyond Networks. In *Proceedings of the 19th ACM International Symposium on Mobility Management and Wireless Access*, 11-16.

[8] Albreem, M. A., Juntti, M. and Shahabuddin, S. (2019). Massive MIMO detection techniques: A survey. *IEEE Communications Surveys & Tutorials*, *21*(4): 3109-3132.

[9] Nguyen, M. (2018). Massive MIMO: a survey of benefits and challenges. *ICSES Trans. Comput. Hardw. Electr. Eng*, *4*: 1-4.

[10] Arsal, A., Civanlar, M. R. and Uysal, M. (2021). Coverage analysis of downlink MU-MIMO cellular networks. *IEEE Communications Letters*, *25*(9): 2859-2863.

[11] Kinol, A. M. J., Nisha, A. S. A., Marshiana, D. and Krishnamoorthy, N. R. (2022). Hybrid Multi Beamforming and Multi-User Detection Technique for MU MIMO System. *Wireless Personal Communications*, *124*(4): 3375-3385.

[12] Zhang, W. and Jiang, S. (2021). Effect of node mobility on MU-MIMO transmissions in mobile Ad Hoc networks. *Wireless Communications and Mobile Computing*, *2021*: 1-9.

[13] Spencer, Q. H., Peel, C. B., Swindlehurst, A. L. and Haardt, M. (2004). An introduction to the multi-user MIMO downlink. *IEEE communications Magazine*, *42*(10): 60-67.

[14] Lee, T., Kim, H. S., Park, S. and Bahk, S. (2014, June). Mitigation of sounding pilot contamination in massive MIMO systems. In *2014 IEEE International Conference on Communications (ICC)*, 1191-1196.

[15] Hassan, A. K., Moinuddin, M., Al-Saggaf, U. M., Aldayel, O., Davidson, T. N. and Al-Naffouri, T. Y. (2020). Performance analysis and joint statistical beamformer design for multi-user MIMO systems. *IEEE Communications Letters*, *24*(10): 2152-2156.

[16] Huh, M., Yu, D. and Park, S. H. (2021). Signal processing optimization for federated learning over multi-user MIMO uplink channel. In *2021 International Conference on Information Networking (ICOIN)*, 495-498.

[17] Masud, A. A., Uchechukwu, O. D., Adikpe, A. O.and Ibikunle, F. (2023). Mitigating Interference and Improving the SINR in a Discrete Time Frame of a Downlink MU-MIMO Transmission in 5G and Beyond Wireless Networks. In *2023 International Conference on Science, Engineering and Business for Sustainable Development Goals (SEB-SDG)*, 1: 1-6.